Effect of crumb rubber on engineering properties of fly ash-slag based engineered geopolymer composites

Hui Zhong, Alzain AlHuwaidi, Yihan Zhang, Mingzhong Zhang*

Department of Civil, Environmental and Geomatic Engineering, University College London, London WC1E 6BT, UK

Abstract: Utilising crumb rubber from waste tyres to replace silica sand in engineered geopolymer composites (EGC) can reduce the environmental impact caused by landfilling and burning the tyres as well as that induced by exhausting the natural resources. This paper presents a systematic study on the effect of partially replacing silica sand with crumb rubber (10-40%) on the engineering properties of EGC, with special focus on deflection-hardening behaviour. Results indicate that the workability, density, ultrasonic pulse velocity, drying shrinkage resistance, and compressive and flexural strengths of EGC drop with the increasing crumb rubber content. Regardless of crumb rubber content, all studied EGC mixes exhibit pronounced deflection-hardening and multiple cracking characteristics. Replacing 10% of silica sand with crumb rubber can lead to acceptable compressive and flexural strengths of EGC. The crack width of EGC containing crumb rubber after flexural loading ranges from around 39 μm to 68 μm, which is lower than that of EGC with silica sand only. The presence of crumb rubber can lead to more PVA fibres pulled out and the rubber at the cracking interface may contribute to restraining the crack growth, which is conducive to improving the flexural toughness of EGC and reducing crack width.

Keywords: Fibre reinforced concrete; Geopolymer; Engineered cementitious composites; Crumb rubber; Toughening mechanism; Sustainability

1. Introduction

Engineered cementitious composites (ECC) were developed in the early 1990s to overcome the brittleness of normal cementitious materials, which possess extraordinary tensile ductility and multiple cracking characteristics [1]. The induced crack width of ECC during the strain-hardening stage is around or lower than 100 μm, which is much smaller as compared with normal concrete [2]. It is worth noting that the Portland cement content in a typical ECC is about 2-3 times higher than that in ordinary concrete, which makes ECC not sustainable as the manufacture of Portland cement is a major contributor to global CO_2 emissions (around 8%) [3, 4]. Therefore, an increasing number of studies have been focused on the development of greener and more sustainable ECC in the last decade.

Geopolymers synthesised through the alkali activation of industrial by-products (e.g., fly ash) are regarded as a promising alternative to Portland cement considering various aspects such as lower

* Corresponding author. E-mail address: mingzhong.zhang@ucl.ac.uk (M. Zhang)

carbon emissions and more superior engineering properties [5]. Given the potential benefits of utilising geopolymers in the construction industry, many attempts have been made to replace Portland cement in ECC with geopolymers, aiming to develop green, sustainable and highly ductile fibre reinforced geopolymer composites, called engineered geopolymer composites (EGC) [6]. Different precursors have been used to develop EGC, such as fly ash, ground granulated-blast furnace slag and metakaolin [7-10]. Among all available EGC mixes, the one adopting blended fly ash and slag as the precursor has attracted much attention in recent years as it can attain a good synergy between fresh and hardened properties under ambient temperature [11-13], which is more suitable for cast-in-situ applications along with reduced cost and energy consumption.

It was estimated that around 1000 million waste tyres are generated annually and more than half of them are landfilled [14]. This number may rise to 1200 million yearly by the year 2030. Apart from landfilling, fire burning is also a disposal way for these end-of-life tyres, while both methods can pose many types of environmental risks [15]. Hence, it is important and urgent to propose an appropriate solution to dispose of this huge number of waste tyres every year. Through mechanical shredding of tyres under ambient temperature, cryogenic degradation of tyres or thermal degradation of tyres, several materials especially rubber particles with various sizes can be retrieved, e.g., crumb rubber [16, 17]. Depending on the size of these rubber particles, they can be incorporated into concrete to partially or fully replace aggregates and cement [18]. This process can help reduce the environmental impacts caused by landfilling and burning waste tyres and the overexploitation of natural resources. It was reported that the incorporation of crumb rubber into cement-based materials can improve the cracking resistance and durability as well as the energy absorption capacity under dynamic loading [19-22].

In recent years, crumb rubber has also been utilised to partly replace silica sand in ECC to improve its sustainability. It was generally found that the tensile strain capacity or flexural deformation capacity of ECC can be improved in the presence of crumb rubber [23-30], which can be attributed to the decreased matrix toughness and interface bonding as well as the increasing number of active flaws [31]. In addition, crumb rubber contributed to reducing the crack width of ECC [32]. For instance, the crack number, crack spacing and crack width of ECC were changed from 16 to 58, 5.04 mm to 1.37 mm, and 155 μm to 116 μm, respectively when 50% of Portland cement was replaced with crumb rubber [29]. It was also reported that incorporating crumb rubber into ECC can enhance its resistance against impact loading [25, 28]. However, most of these studies found that the mechanical strengths of ECC such as compressive and tensile strengths were weakened in the presence of crumb rubber. Some of them indicated that the drying shrinkage of ECC containing crumb rubber was higher than that of normal ECC [23, 27, 30]. Up to now, to the author's best knowledge, only one study [33] has explored the effect of crumb rubber on the mechanical properties of slag-

based EGC, revealing that the inclusion of crumb rubber greatly improved the tensile strain capacity of EGC although the tensile and compressive strengths dropped. Adopting crumb rubber to substitute 5% of slag can achieve a superior tensile strain-hardening behaviour along with very tight crack widths (73.2 μm). Although the above study proved the feasibility of using crumb rubber in EGC, the effect of crumb rubber as alternative sand on the overall behaviour of EGC is still unclear. It is worth noting that the interfacial transition zone would significantly affect the mechanical properties and durability of EGC [34]. As mentioned earlier, fly ash-slag based EGC has many benefits over either fly ash- or slag-based EGC. Thus, it is vital to study the role of crumb rubber in engineering properties of fly ash-slag based EGC.

The main purpose of this study is to investigate the effect of partial replacement of silica sand with crumb rubber (10-40%) on the engineering properties of EGC. The EGC mix made from silica sand alone was prepared and used as the reference. A series of experimental tests including workability, density, ultrasonic pulse velocity (UPV), compressive strength and four-point bending tests were carried out. Regarding the four-point bending test, the stress-displacement response, failure mode, cracking behaviour, flexural strength and flexural toughness of EGC with and without crumb rubber were discussed in depth. The fibre condition across the cracking interface was also explored to understand the underlying mechanisms.

2. Experimental program

2.1 Raw materials

Low-calcium fly ash and ground granulated blast-furnace slag were used as the precursors of EGC, the chemical compositions and particle size distribution of which are presented in Table 1 and Fig. 1, respectively. Silica sand with a specific gravity of 2.65 and crumb rubber obtained from the ambient grinding of truck tyres with a specific gravity of 1.14 were adopted as the aggregates in the mixtures. The particle size distribution of silica sand and crumb rubber is also shown in Fig. 1. As per the previous studies [12, 35], a mixture of NaOH solution (10 M) and Na_2SiO_3 solution with a silicate modulus of 2.58 was used as alkaline activator, where NaOH solution was prepared by dissolving 400 g of NaOH pellets in one litre of solution. A polycarboxylate-based superplasticiser was incorporated into the mixtures to adjust their workability. PVA fibre with a length of 12 mm and a diameter of 40 μm supplied by Kuraray Co., Ltd., Japan was used for all proposed mixes in this study. The tensile strength and elastic modulus of the used PVA fibre are 1600 Mpa and 41 GPa, respectively.

Table 1 Chemical compositions (wt.%) of fly ash and ground granulated blast-furnace slag.

Type/oxide	SiO_2	Al_2O_3	CaO	Fe_2O_3	MgO	K_2O	MnO
Fly ash	49.80	25.08	4.65	11.67	1.67	3.30	-
Slag	34.10	12.30	44.20	0.41	8.12	0.56	0.25

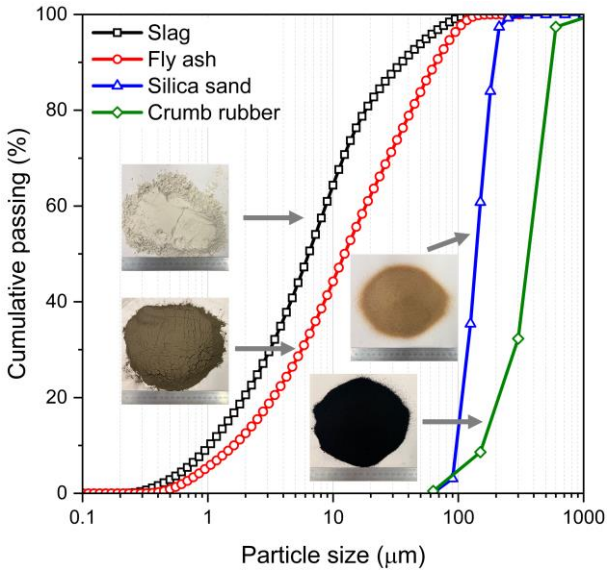

Fig. 1. Particle size distribution of fly ash, slag, silica sand and crumb rubber.

2.2 Mix proportions

Table 2 lists the mix proportions of studied EGC mixes. The mass ratios of fly ash/slag, activator/precursor, silica sand/precursor, and superplasticiser/precursor were set as 4.0, 0.4, 0.2, and 0.01, respectively based on previous studies [12, 36]. In addition, the PVA fibre volume fraction in all mixtures was 2.0%. The silica sand was substituted with crumb rubber at an increment of 10% up to 40%. It was reported that the compressive strength of ECC was decreased by about 26% when 50% of silica sand was replaced with crumb rubber [23]. Besides, around a 90% reduction in compressive strength was observed for normal concrete when 40% crumb rubber was used to substitute the dune sand [37]. Therefore, the highest crumb rubber replacement level was set as 40% to ensure the proposed mixtures possess acceptable mechanical properties. Regarding the mix ID, CR0 indicates the mixture without any addition of crumb rubber while CR10 denotes the mixture containing 10% crumb rubber.

Table 2 Mix proportions of EGC (kg/m^3).

Mix ID	Fly ash	Slag	NaOH	Na_2SiO_3	Silica sand	Crumb rubber	Superplasticiser	PVA
CR0	994	248.5	165.7	331.4	248.5	0	12.4	26
CR10	994	248.5	165.7	331.4	223.7	24.9	12.4	26
CR20	994	248.5	165.7	331.4	198.8	49.7	12.4	26
CR30	994	248.5	165.7	331.4	174	74.6	12.4	26
CR40	994	248.5	165.7	331.4	149.1	99.4	12.4	26

2.3 Sample preparation

All samples were prepared using a Hobart mixer in this study. Fly ash, slag, silica sand and crumb rubber (if any) were first mixed for 2 min. Then, the alkaline activator was slowly added to the mixture and mixed for 3 min followed by the addition of superplasticiser. After another 1 min of mixing, PVA

fibres were slowly and carefully added to the mixture to ensure uniform fibre dispersion. The mixing was continued for another 1 min when all PVA fibres were uniformly added into the mixture. The total mixing time of all mixtures was around 12 min. Upon the completion of mixing, the fresh samples were poured into moulds with various sizes. All specimens were de-moulded after 24 h and then moved into a curing room with constant temperature and relative humidity of around 20 ^{o}C and 50% until the testing ages.

2.4 Testing methods

The flow table test was used to assess the workability of all EGC mixes as per ASTM C1437-15 [38]. For each mix ID, the flow table test was repeated three times. 50 mm cubic samples were utilised for determining the density [39] and UPV value of EGC at 7 d and 28 d. UPV is a non-destructive technique to indirectly reflect the quality of the test specimen based on the required velocity for an ultrasonic pulse to pass through the sample. Fig. 2 illustrates the UPV test setup, where the direct transmission was used during the test. For each mixture, six samples were tested for both density and UPV. The drying shrinkage of EGC was evaluated by measuring the length change of the prismatic sample (50 mm × 50 mm × 285 mm) between the de-moulding day and subsequent curing days. For each mix, three specimens were tested.

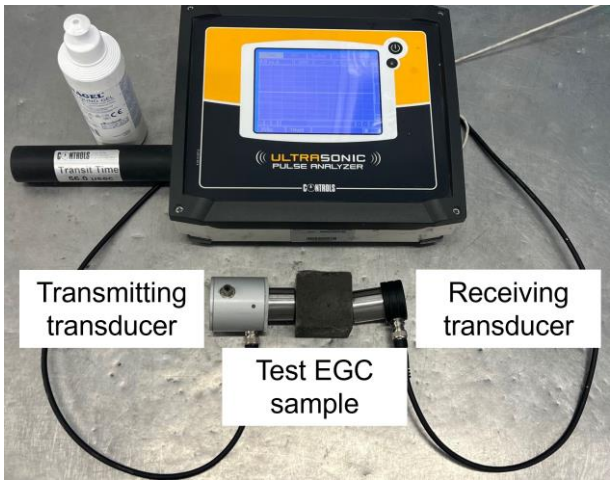

Fig. 2. A photo of UPV test apparatus.

The samples used for the density and UPV tests were then adopted for measuring the compressive strength according to ASTM C109/C109M-20b [40]. A constant loading rate of 1200 N/s was used for all test specimens. The four-point bending test was performed as per ASTM C1609 [41] to characterise the flexural behaviour of EGC, the test setup of which is shown in Fig. 3. The used specimen size was 20 mm × 100 mm × 400 mm and the test loading span was set as 300 mm. Three specimens were prepared and tested for each mix ID. A dial gauge was installed to measure the mid-span deflection of the test sample and the whole loading process was recorded to help obtain the deflection results. After each test, the residual crack number and crack width in the upper, middle and lower lines of the tested specimen were measured using a portable microscope (Dino-Lite Edge

AM73115MZT), as illustrated in Fig. 4 [42]. For the crack across more than one line, its crack width was determined by averaging the crack width in each line. The microscope was also applied to explore the cracking interface to understand the inherent mechanisms.

Fig. 3. A photo of four-point bending test setup.

Fig. 4. An example of how to determine the crack number and crack width of EGC.

3. Results and discussion

3.1 Workability

Fig. 5 presents the effect of crumb rubber content on the workability of EGC, which indicates a conspicuous trend that the flow value of EGC dropped with the increasing crumb rubber content. For instance, replacing 30% of silica sand with crumb rubber reduced the flow value by about 37%, which can be ascribed to the irregular shape and rough surface texture of rubber particles as compared with silica sand particles [43, 44]. Previous studies reported a similar phenomenon for cement-based materials [45, 46] and geopolymers [47, 48]. As mentioned previously, most rubber particles are recovered from the mechanical shredding process of waste tyres and the surface texture of the crumb

rubber is highly dependent on the manufacturing process. Some studies found that the workability of geopolymers was improved in the presence of crumb rubber due to the relatively smooth surface texture of crumb rubber compared to sand or the presence of more free water caused by the hydrophobicity of crumb rubber [49, 50]. The fibre content would also affect the workability of EGC with crumb rubber as the interaction between the constituent materials could be intensified when the incorporated fibre dosage is too high.

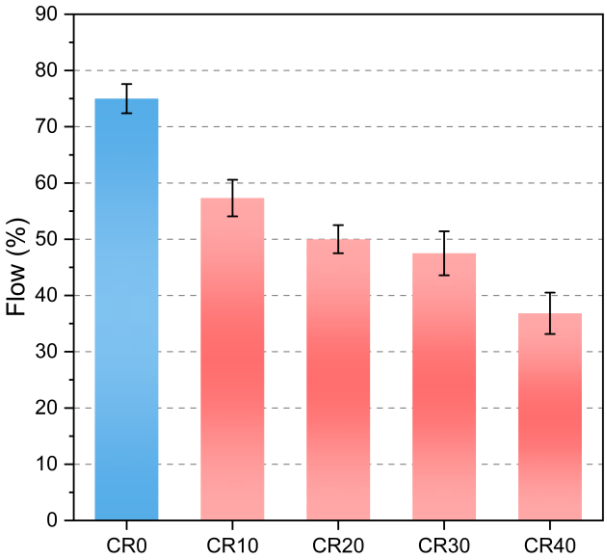

Fig. 5. Flowability of EGC mixes containing various crumb rubber contents.

3.2 Density and ultrasonic pulse velocity

The effect of crumb rubber content on the density of EGC is illustrated in Fig. 6a. Regardless of curing age, the density of EGC containing crumb rubber was lower than that of EGC with silica sand only. The density of CR10, CR20, CR30 and CR40 at 7 d was 3.98%, 5.65%, 6.83% and 7.04% respectively smaller than that of the reference mix (CR0), which can be primarily attributed to the lower specific gravity of crumb rubber (1.14) in comparison with silica sand (2.65). The rise of air content inside EGC due to the presence of crumb rubber can also contribute to the reduction of density [51]. A similar finding was reported by Lương et al. [33] that the density of crumb rubber EGC was 5-10% lower than that of the mix without crumb rubber. It is interesting to note that the differences in density between EGC with and without crumb rubber at 28 d (about 2-5%) were smaller than those at 7 d, which can be associated with the reaction between extra NaOH solution and some components of rubber (e.g., isoprene), reducing the entrapped air content [52]. Comparative results were reported in previous studies that the density of geopolymers [53] or cement-based concrete [54] containing NaOH-treated crumb rubber was higher than those of mixes incorporating as-received crumb rubber.

Fig. 6b shows the UPV values of all mixes. A higher UPV value generally indicates a better quality of the test specimen and a lower number of internal flaws inside the sample. The UPV values of all EGC mixtures at 7 d and 28 d ranged from 3064 km/s to 3310 km/s and 3087 km/s to 3333 km/s, respectively, implying that the change of curing age did not have an apparent effect on the UPV of

EGC. Similar to the trend of density, the UPV of EGC went down with the increasing crumb rubber content. For instance, the UPV value of CR40 at 28 d was around 7% lower than that of CR0. Similar results were captured in previous studies on ECC [23], geopolymers [55] and cement-based concrete [43]. The main reason can be associated with the increased porosity for EGC due to the addition of crumb rubber. Ultrasonic pulses travel through solid materials faster than through porous materials [56] and thus, a longer travel time is required for the pulse to pass through the specimen containing crumb rubber.

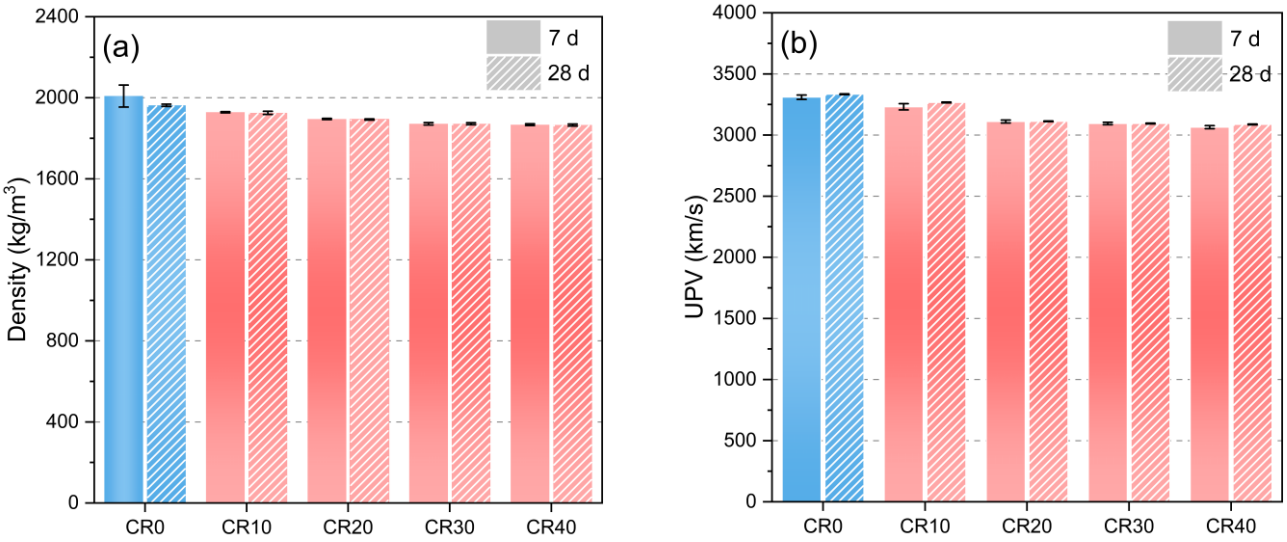

Fig. 6. Effect of crumb rubber content on (a) density and (b) UPV of EGC.

3.3 Drying shrinkage

Similar to ECC, coarse aggregates are typically excluded in the mix design of EGC as they can increase the matrix toughness and weaken the tensile strain-hardening behaviour of EGC [6]. As a result, the drying shrinkage resistance of EGC would be lower than that of normal concrete since the excellent shape stability of coarse aggregates can effectively restrain the drying shrinkage. It was reported that fly ash-slag based geopolymers had higher drying shrinkage than cement-based pastes, mainly due to the higher mesopore volume of geopolymers relative to cementitious pastes [57]. Thus, it is essential to study the effect of crumb rubber content on the drying shrinkage of EGC to ensure it has acceptable durability.

The drying shrinkage of all EGC mixes at different curing ages is shown in Fig. 7, indicating that the drying shrinkage of EGC developed very rapidly at early ages and gradually slowed down with the increase of curing age. Generally, the drying shrinkage of EGC with crumb rubber was higher than that of EGC without crumb rubber although there was no clear trend when the crumb rubber content varied. Within the first 21 d, the drying shrinkage of CR0 was comparable to that of CR10. After that, EGC containing crumb rubber had similar drying shrinkage but larger than the reference mixture. For instance, the drying shrinkage of CR10, CR20, CR30 and CR40 at 28 d was 0.646%, 0.682%, 0.660% and 0.670%, respectively, which was 9.58-15.76% greater than that of CR0. This

can be attributed to the reduced internal restraint to shrinkage caused by the lower elastic modulus of crumb rubber compared to silica sand and the increased rate of moisture loss due to higher porosity in the presence of crumb rubber [46, 58]. It agrees well with the literature finding [23, 27, 50] that the drying shrinkage of ECC or geopolymers went up with the increase of sand replacement by crumb rubber.

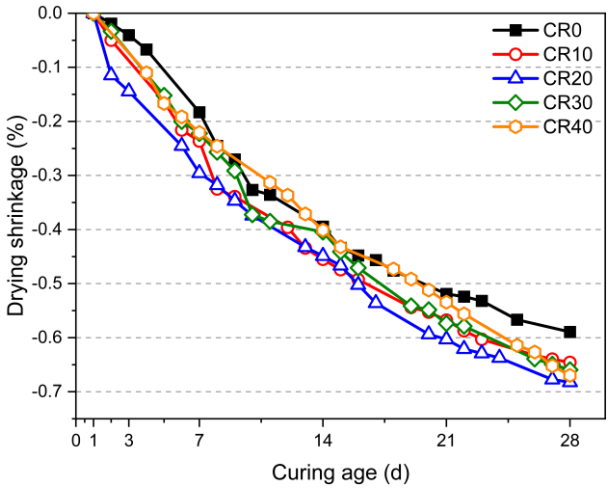

Fig. 7. Drying shrinkage of EGC with various crumb rubber contents at different curing ages.

3.4 Compressive strength

Fig. 8 displays the compressive strength of EGC with various crumb rubber contents at 7 d and 28 d, indicating that CR0 held the highest compressive strengths of 29.2 MPa and 52.4 MPa, respectively. Irrespective of curing age, the presence of crumb rubber lowered the compressive strength of EGC and the reduction was higher when more silica sand was replaced with crumb rubber. The 28-d compressive strengths of CR10, CR20, CR30 and CR40 were approximately 8%, 24%, 33% and 43% lower than that of CR0, which is consistent with most of the existing studies on cementitious and geopolymer materials. It can be explained by the fact that: (1) the non-homogeneity of EGC tends to be higher in the presence of crumb rubber owing to the reduced workability and increased entrapped air content; (2) the compressive cracks are more likely to appear near the crumb rubber as the crumb rubber can be deformed more easily due to its lower stiffness [59, 60]; (3) the weak bonding between the crumb rubber and the matrix [18]; (4) some rubber particles may be damaged by NaOH solution with a high concentration [61]. However, the reaction between NaOH solution and crumb rubber can mitigate the negative effect on compressive strength of EGC as NaOH can accelerate the oxidative decomposition of crumb rubber, forming the carboxyl groups with Na^+ and thus the wettability of crumb rubber [54, 62]. This can promote cement hydration, enhancing the compressive strength of EGC. Hence, when the sand replacement dosage by crumb rubber in EGC was appropriate (e.g., 10%), EGC could still have an acceptable compressive strength. Previous studies revealed that the compressive strength of cement-based and geopolymer mixes was significantly improved when the used crumb rubber particles were soaked in NaOH solutions for 40 min [49, 54]. Moreover, a previous

study [62] found that crumb rubber can be simultaneously treated during the alkali-activation process of geopolymers to reduce the negative effects of crumb rubber on the properties of geopolymers, implying that no pre-treatment of crumb rubber is needed before the mixing.

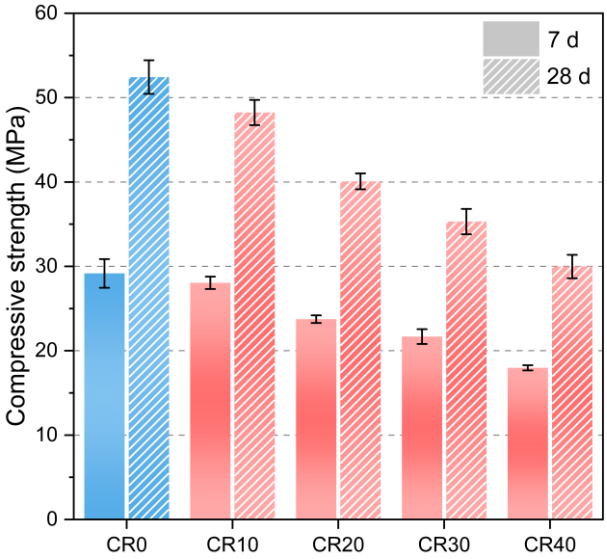

Fig. 8. Effect of crumb rubber content on compressive strength of EGC.

The typical compressive failure patterns of EGC are shown in Fig. 9. Varying the sand replacement dosage by crumb rubber did not significantly change the failure pattern of EGC. All mixtures retained the original shape of test specimens along with vertical macrocracks parallel to the loading direction. Owing to the fibre bridging effect, the lateral expansion of specimens was effectively restrained.

Fig. 9. Typical compressive failure patterns of EGC with various crumb rubber contents at 28 d.

The density and UPV of EGC can be correlated with the compressive strength, the results of which are presented in Figs. 10a and 10b, respectively. As seen in Fig. 10a, the density of EGC at both 7 d and 28 d had positive correlations with compressive strengths, which is consistent with the literature on slag-based EGC [33], ECC [23, 63] and fly ash-slag based geopolymer concrete [50]. It can be ascribed to the densified microstructure along with lower porosity when the density of the specimen is higher. Fig. 10b indicates a similar trend that the UPV of EGC was positively correlated with the compressive strength. The relation between UPV and compressive strength can be described as follows [64]:

$$f_c = Ae^{B \cdot UPV} \quad (1)$$

where A and B are the constant coefficients.

The fitted exponential curves of EGC at 7 d and 28 d are presented in Fig. 10b, which can be considered as reliable models since the equations had a R^2 of over 0.8 [65], and thus can be used to estimate the change of deterioration level of EGC with time. The rising rate of compressive strength with the change of UPV at 28 d was slightly higher than that at 7 d, which was also observed in previous studies [23, 55]. Adesina and Das [23] proposed a linear equation to describe the relation between UPV and compressive strength with a R^2 of 0.9897:

$$f_c = 0.022UPV - 33.78 \quad (2)$$

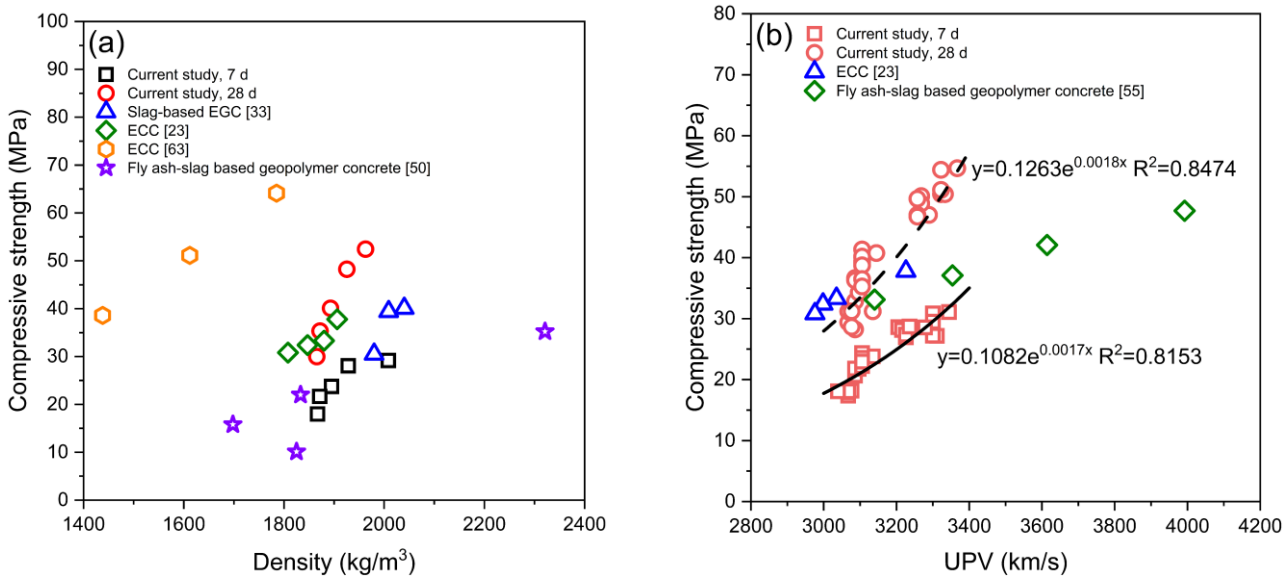

Fig. 10. Compressive strength of EGC against its (a) density and (b) UPV.

3.5 Flexural behaviour

The flexural behaviour of EGC in terms of stress-deflection relationship, failure pattern and cracking behaviour, flexural strength, and flexural toughness was analysed and discussed in this section.

3.5.1 Stress-deflection response

Fig. 11 depicts the stress-deflection relationship of all EGC mixes, indicating that they exhibited a pronounced deflection-hardening behaviour under four-point bending. The stress-deflection curves mainly consisted of two stages. In the first stage, the flexural stress of EGC was linearly increased up to the elastic limit, where the first crack was initiated at that point. The first crack of the test specimen was mainly induced by the existence of initial flaws when the load went up. Then, the stress-deflection curve of the specimen entered into the deflection-hardening stage and the curve showed some stress drops forming several serrated lines. These stress drops denoted the formation of microcracks and a larger drop typically indicated a larger crack opening. More serrated lines can be observed for EGC containing fewer crumb rubber while the stress-deflection curves of EGC with more crumb rubber (CR30 and CR40) were smoother during the deflection-hardening stages, suggesting that increasing the sand replacement level by crumb rubber may lower the crack width under four-point bending. A similar observation was found in a previous study [27].

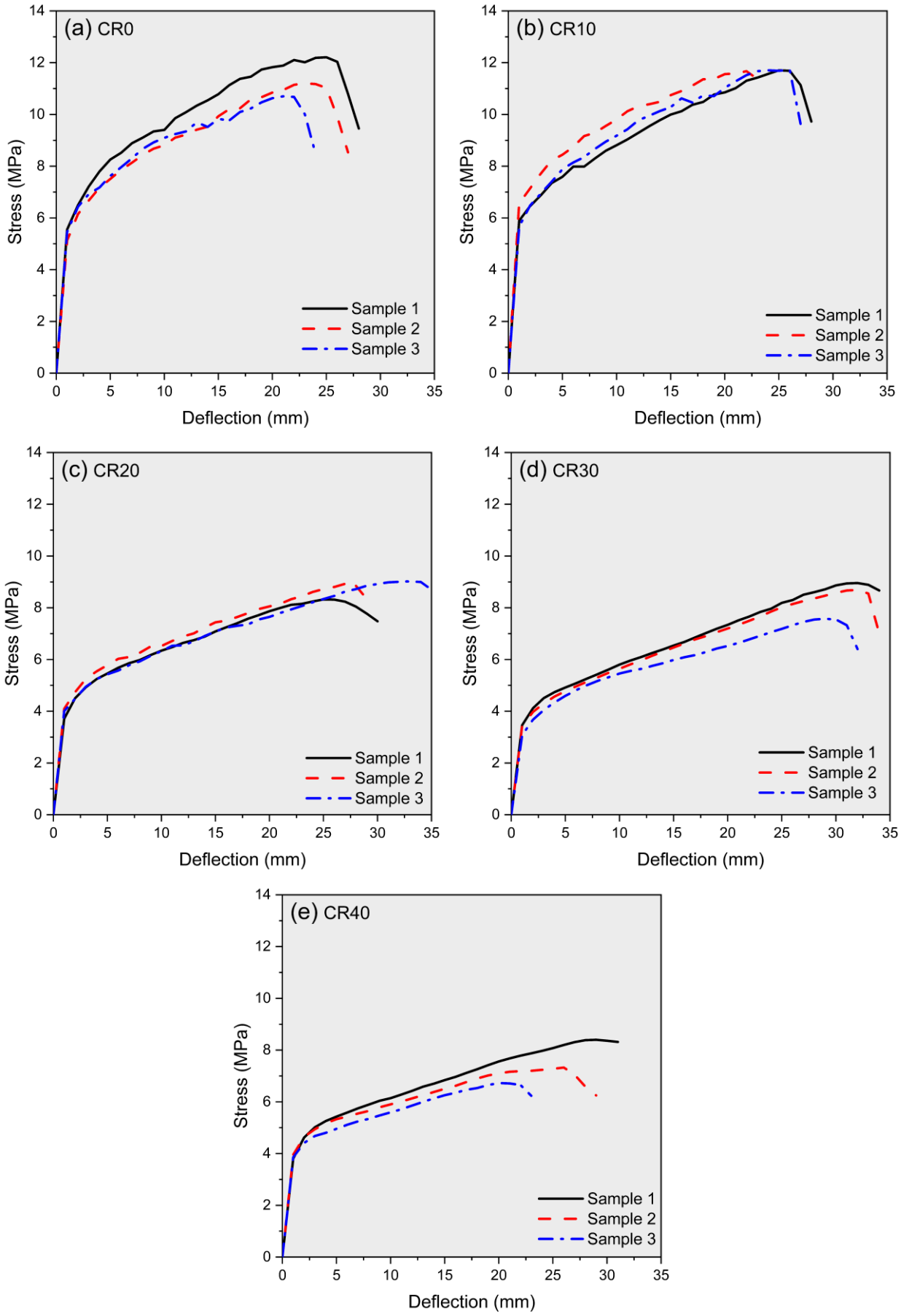

Fig. 11. Flexural stress-deflection response of EGC with various crumb rubber contents.

3.5.2 Failure pattern

Fig. 12 demonstrates the typical microcracks formed over the tensile side of EGC containing crumb rubber from two different views. Consistent with the stress-deflection curves shown in Fig. 11, multiple microcracks along with a main major crack can be observed and the specimen behaved like a bendable slab instead of experiencing sudden failure. The cracking patterns of all EGC mixes after the four-point bending are illustrated in Fig. 13.

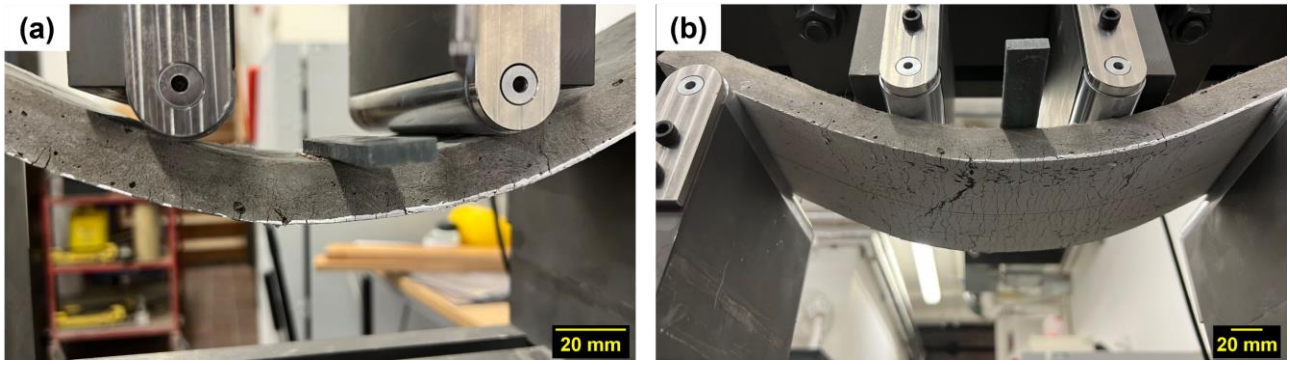

Fig. 12. Typical microcracks on the tensile side of CR10: (a) front view and (b) bottom view.

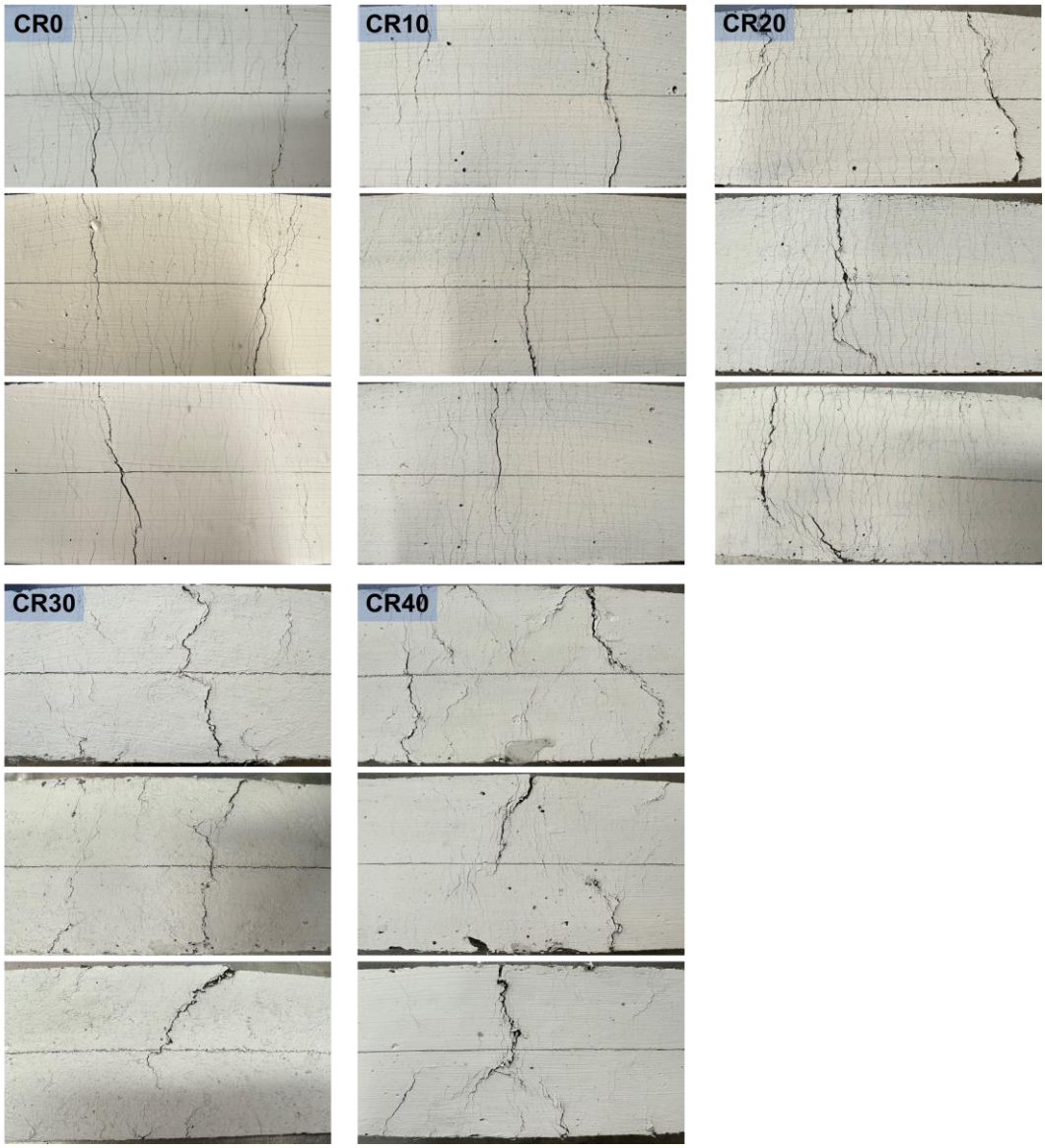

Fig. 13. Typical failure patterns of EGC with various crumb rubber contents.

It should be noted that these images were taken immediately after unloading and some very tight cracks may be closed and were difficult to detect [66]. Based on visual observation, multiple microcracks can be captured for all mixtures while such behaviour was more conspicuous for CR0, CR10 and CR20. This agrees well with the discussion in the last section that the crack widths of CR30 and CR40 were tighter. Some of these tight crack widths were enlarged using a portable microscope (see Fig. 14). After unloading each failed specimen, its crack number and crack width were measured although the residual crack width could not fully represent the crack width of the specimen during the flexural loading. The result can still be used to evaluate the effect of crumb rubber on the cracking performance of EGC below.

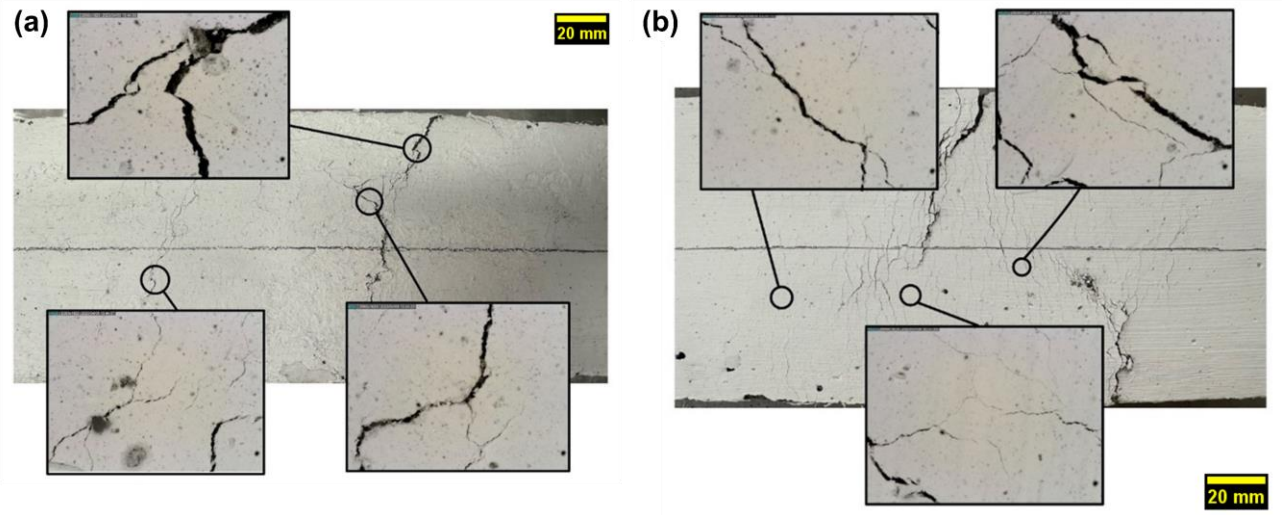

Fig. 14. Examples of tight microcracks in (a) CR30 and (b) CR40.

3.5.3 Cracking analysis

Fig. 15 displays the residual crack number and crack width of EGC against crumb rubber content. Increasing the crumb rubber content to 20% did not significantly vary the crack number of EGC while the further increments to 30% and 40% increased the crack number of EGC by about 36% and 43%, respectively. On the other hand, the residual crack width of EGC gradually dropped with the rising sand replacement level by crumb rubber. For instance, the average crack width of CR40 was 38.92 μm which was around 44% lower than that of CR0. Similar findings were reported when crumb rubber was used to replace silica sand in ECC [27, 32]. The rise in crack number and reduced crack width for EGC caused by the presence of crumb rubber can be ascribed to the following reasons: (1) crumb rubber particles can weaken the matrix toughness due to their lower stiffness to lower the stress level needed to induce a new crack [31]; (2) more active flaws can be introduced by the addition of crumb rubber to improve the microcrack density and thereby the ductility [1]; (3) crumb rubber particles may bridge the microcracks to restrain the crack width [32]. Nevertheless, a previous research study [33] reported an inconsistent finding that adding 5% crumb rubber into slag-based

EGC increased the crack number and reduced the crack width, whereas the further addition of crumb rubber to 10% led to opposite effects. This may be associated with the poor interfacial bonding between fibres and the matrix and the bridging fibres can be pulled out very quickly before the formation of a new crack, resulting in localisation of failure.

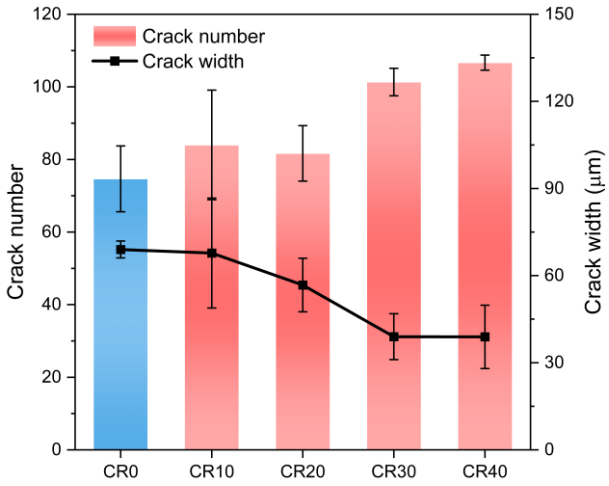

Fig. 15. Effect of crumb rubber content on residual crack number and crack width of EGC.

Fig. 16 shows the fibre conditions at the crack interfaces of CR0, CR10 and CR40 after four-point bending tests. Both fibre pull-out and fibre rupture can be observed at the crack interface of EGC with no crumb rubber (CR0). It should be noted that fibre pull-out is more favourable for improving the flexural deformation capacity of EGC. As mentioned above, the interfacial bonding of fibre and matrix would be weakened due to the presence of crumb rubber and therefore, the fibres would tend to be pulled out. More pulled out PVA fibres appeared at the crack interfaces of CR10 and CR40. In addition, some rubber particles can be found at the cracking interfaces, implying that they could bridge the microcrack to restrain its crack width as the flexural loading goes up. As crumb rubber is an elastomer, it can sustain a large deformation when the microcrack grows until rupturing [32].

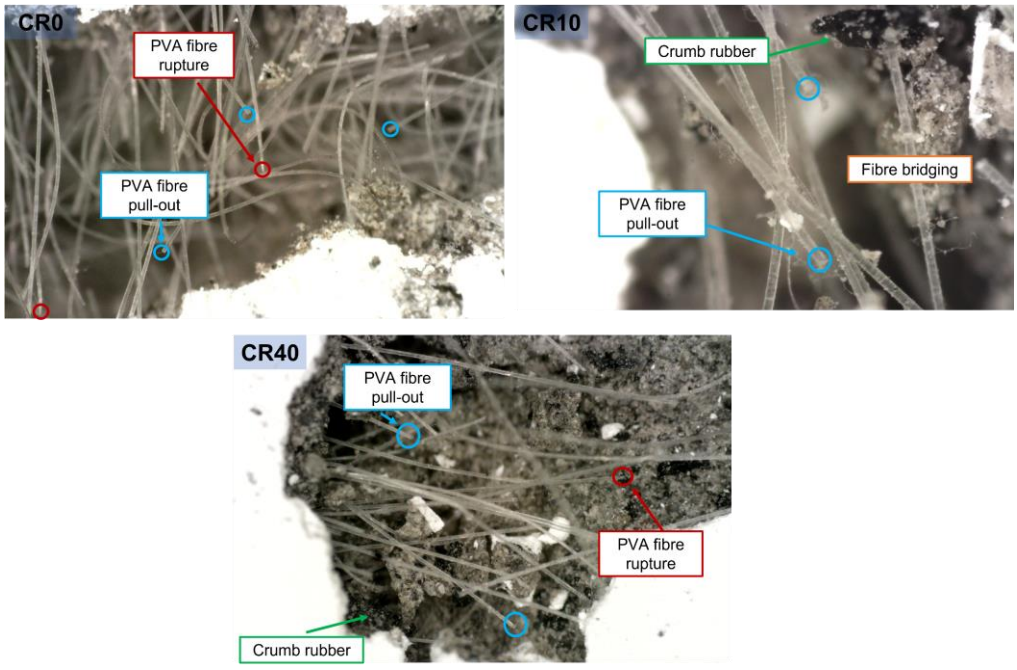

Fig. 16. Fibre conditions across the cracking interfaces in EGC.

3.5.4 Flexural strength and toughness

Fig. 17a presents the flexural strength of EGC with various crumb rubber contents. Different from compressive strength (Fig. 8), replacing 10% of silica sand with crumb rubber did not weaken the flexural strength of EGC. However, when 20% of silica sand was substituted with crumb rubber, the flexural strength of EGC was dropped by approximately 23%, while the further increase of crumb rubber replacement content to 30% and 40% did not considerably reduce the flexural strength of EGC. The reasons causing this reduction are similar to those explained for the compressive strength (see Section 3.4). When the incorporated crumb rubber content was appropriate (10%), the reaction between NaOH solution and crumb rubber can improve the bonding between crumb rubber and matrix, minimising the negative effect of crumb rubber on the flexural strength of EGC. PVA fibres played a more essential role in flexural strength than in compressive strength. Therefore, combining PVA fibres and crumb rubber with improved wettability would not considerably lower the flexural strength of EGC. Previous studies [23, 27] also revealed that the reduction in flexural strength of ECC caused by the crumb rubber was lower than that in compressive strength. For instance, replacing 50% of silica sand with crumb rubber reduced the compressive strength of ECC by 26.1% while it only reduced the flexural strength by 10.5% [23].

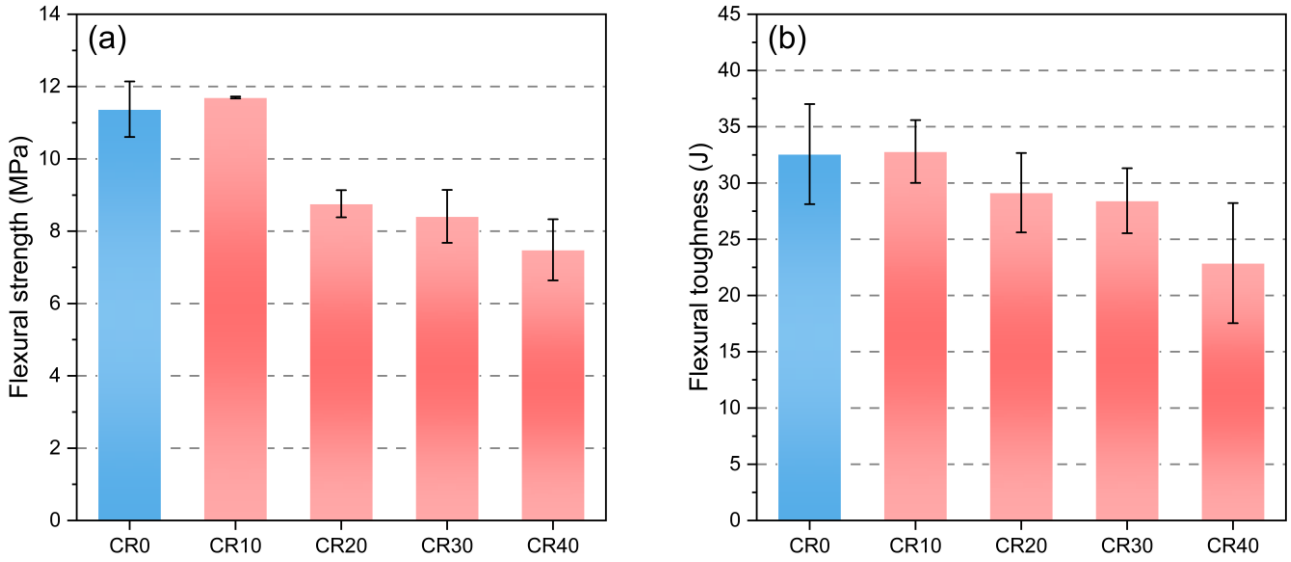

Fig. 17. Effect of crumb rubber content on (a) flexural strength and (b) toughness of EGC.

The flexural toughness of ECC in this study was determined by integrating the load-deflection curve, the results of which are illustrated in Fig. 17b. The flexural toughness defined in ASTM C1609 [41] can be calculated as the area enclosed under the load-deflection curve up to the point of the mid-span deflection of 2 mm, which was not adopted herein since it could not fully understand the toughness of the mixture with a superior deflection-hardening behaviour. Except for CR40, the flexural toughness of CR10, CR20 and CR30 ranged from 28.42 J to 32.80 J, which was comparable to CR0 (32.57 J). As discussed in Section 3.5.3, incorporating the crumb rubber into ECC can promote

the PVA fibre pull-out that can benefit the toughness of the specimen. More microcracks were generated when more silica sand was substituted with crumb rubber, enhancing the flexural toughness of ECC. The crumb rubber can absorb more energy under deformation owing to its elastic property [23, 62]. These effects can compensate for the loss of toughness induced by reduced flexural strength.

4. Conclusions

In this paper, a systematic experimental study was conducted to explore the effect of replacing silica sand with crumb rubber (10-40%) on the engineering properties of fly ash-slag based engineered geopolymer composites (EGC). Based on the results obtained, the following conclusions can be made:

- Increasing the crumb rubber content reduced the workability, density and ultrasonic pulse velocity of EGC, primarily due to the irregular particle size and lower density of crumb rubber and increased air content inside EGC. The drying shrinkage of EGC with crumb rubber was generally higher than that of EGC with silica sand only, where the drying shrinkage of CR10, CR20, CR30 and CR40 at 28 d was 9.58-15.76% greater than that of CR0.
- The compressive strength of all EGC mixes herein ranged from about 30 MPa to 52 MPa, which is appropriate for engineering applications. The compressive strength of EGC was gradually weakened when silica sand was partly replaced with crumb rubber. The reaction between NaOH solution and crumb rubber may mitigate such negative effect on the compressive strength and thus, replacing 10% of silica sand with crumb rubber can still lead to an acceptable compressive strength for EGC. EGC with or without crumb rubber maintained the structural integrity after compression. There existed a good correction between the density or ultrasonic pulse velocity of all EGC mixtures with compressive strength.
- All studied EGC mixes exhibited clear deflection-hardening and multiple cracking characteristics. The crack number and crack width of EGC after flexural loading were increased and reduced, respectively, in the presence of crumb rubber. For instance, the average crack width of CR40 was 38.92 μm which was around 44% lower than that of CR0. Replacing 20% or more silica sand with crumb rubber weakened the flexural strength of EGC while the flexural toughness was not significantly affected when 10-30% of silica sand was substituted with crumb rubber. The presence of crumb rubber can promote the pull-out of PVA fibre and the crumb rubber across the crack interface can sustain a large deformation as the crack grows, which is beneficial to reducing the crack width of EGC and improving flexural toughness.

Acknowledgements

The authors gratefully acknowledge the financial support from the Engineering and Physical Sciences Research Council (EPSRC) under Grant No. EP/R041504/1 and the Royal Society under Award No. IEC/NSFC/191417. The financial support provided by University College London (UCL) and China Scholarship Council (CSC) to the first author is gratefully acknowledged.

References

[1] V.C. Li, Engineered Cementitious Composites (ECC): Bendable Concrete for Sustainable and Resilient Infrastructure, Springer2019.

[2] V.C. Li, From micromechanics to structural engineering-the design of cementitous composites for civil engineering applications, Journal of Structural Mechanics and Earthquake Engineering 10 (1993) 37-48.

[3] R.M. Andrew, Global CO 2 emissions from cement production, Earth System Science Data 10(1) (2018) 195-217.

[4] T. Luukkonen, Z. Abdollahnejad, J. Yliniemi, P. Kinnunen, M. Illikainen, One-part alkali-activated materials: A review, Cement and Concrete Research 103 (2018) 21-34.

[5] J.L. Provis, J.S.J. Van Deventer, Geopolymers: structures, processing, properties and industrial applications, Elsevier2009.

[6] H. Zhong, M. Zhang, Engineered geopolymer composites: A state-of-the-art review, Cement and Concrete Composites 135 (2023) 104850.

[7] J. Cai, J. Pan, J. Han, Y. Lin, Z. Sheng, Low-energy impact behavior of ambient cured engineered geopolymer composites, Ceramics International 48(7) (2022) 9378-9389.

[8] M. Ohno, V.C. Li, A feasibility study of strain hardening fiber reinforced fly ash-based geopolymer composites, Construction and Building Materials 57 (2014) 163-168.

[9] B.Y. Lee, C.-G. Cho, H.-J. Lim, J.-K. Song, K.-H. Yang, V.C. Li, Strain hardening fiber reinforced alkali-activated mortar – A feasibility study, Construction and Building Materials 37 (2012) 15-20.

[10] J. Cai, J. Pan, J. Han, X. Wang, Mechanical Behaviors of Metakaolin-Based Engineered Geopolymer Composite under Ambient Curing Condition, Journal of Materials in Civil Engineering 34(7) (2022) 04022152.

[11] S. Zhang, V.C. Li, G. Ye, Micromechanics-guided development of a slag/fly ash-based strain-hardening geopolymer composite, Cement and Concrete Composites 109 (2020) 103510.

[12] H. Zhong, M. Zhang, Effect of recycled tyre polymer fibre on engineering properties of sustainable strain hardening geopolymer composites, Cement and Concrete Composites 122 (2021) 104167.

[13] B. Nematollahi, J. Sanjayan, J. Qiu, E.-H. Yang, Micromechanics-based investigation of a sustainable ambient temperature cured one-part strain hardening geopolymer composite, Construction and Building Materials 131 (2017) 552-563.

[14] B.S. Thomas, R.C. Gupta, A comprehensive review on the applications of waste tire rubber in cement concrete, Renewable and Sustainable Energy Reviews 54 (2016) 1323-1333.

[15] W. Shen, L. Shan, T. Zhang, H. Ma, Z. Cai, H. Shi, Investigation on polymer–rubber aggregate modified porous concrete, Construction and Building Materials 38 (2013) 667-674.
[16] K. Pilakoutas, K. Neocleous, H. Tlemat, Reuse of tyre steel fibres as concrete reinforcement, Proceedings of the Institution of Civil Engineers-Engineering Sustainability, Thomas Telford Ltd, 2004, pp. 131-138.
[17] S. Ramarad, M. Khalid, C.T. Ratnam, A.L. Chuah, W. Rashmi, Waste tire rubber in polymer blends: A review on the evolution, properties and future, Progress in Materials Science 72 (2015) 100-140.
[18] E. Ganjian, M. Khorami, A.A. Maghsoudi, Scrap-tyre-rubber replacement for aggregate and filler in concrete, Construction and Building Materials 23(5) (2009) 1828-1836.
[19] A. Turatsinze, S. Bonnet, J.L. Granju, Potential of rubber aggregates to modify properties of cement based-mortars: Improvement in cracking shrinkage resistance, Construction and Building Materials 21(1) (2007) 176-181.
[20] O. Onuaguluchi, N. Banthia, Long-term sulfate resistance of cementitious composites containing fine crumb rubber, Cement and Concrete Composites 104 (2019) 103354.
[21] N. Oikonomou, S. Mavridou, Improvement of chloride ion penetration resistance in cement mortars modified with rubber from worn automobile tires, Cement and Concrete Composites 31(6) (2009) 403-407.
[22] F. Liu, G. Chen, L. Li, Y. Guo, Study of impact performance of rubber reinforced concrete, Construction and Building Materials 36 (2012) 604-616.
[23] A. Adesina, S. Das, Performance of engineered cementitious composites incorporating crumb rubber as aggregate, Construction and Building Materials 274 (2021) 122033.
[24] Y. Wang, Z. Zhang, J. Yu, J. Xiao, Q. Xu, Using Green Supplementary Materials to Achieve More Ductile ECC, Materials 12(6) (2019) 858.
[25] Z. Chen, Y. Liang, Y. Lin, J. Cai, Recycling of waste tire rubber as aggregate in impact-resistant engineered cementitious composites, Construction and Building Materials 359 (2022) 129477.
[26] J. Ye, C. Cui, J. Yu, K. Yu, J. Xiao, Fresh and anisotropic-mechanical properties of 3D printable ultra-high ductile concrete with crumb rubber, Composites Part B: Engineering 211 (2021) 108639.
[27] Z. Zhang, H. Ma, S. Qian, Investigation on Properties of ECC Incorporating Crumb Rubber of Different Sizes, Journal of Advanced Concrete Technology 13(5) (2015) 241-251.
[28] Z. Zhang, F. Qin, H. Ma, L. Xu, Tailoring an impact resistant engineered cementitious composite (ECC) by incorporation of crumb rubber, Construction and Building Materials 262 (2020) 120116.
[29] M. Hou, D. Zhang, V.C. Li, Crack width control and mechanical properties of low carbon engineered cementitious composites (ECC), Construction and Building Materials 348 (2022) 128692.

[30] X. Huang, R. Ranade, W. Ni, V.C. Li, On the use of recycled tire rubber to develop low E-modulus ECC for durable concrete repairs, Construction and Building Materials 46 (2013) 134-141.
[31] D. Shoji, Z. He, D. Zhang, V.C. Li, The greening of engineered cementitious composites (ECC): A review, Construction and Building Materials 327 (2022) 126701.
[32] M. Hou, K. Xu, P.J.M. Monteiro, V.C. Li, Rubber particle bridging effect on crack width control of low carbon Engineered Cementitious Composites (ECC), Cement and Concrete Composites 140 (2023) 105106.
[33] Q.-H. Lương, H.H. Nguyễn, J.-I. Choi, H.-K. Kim, B.Y. Lee, Effects of crumb rubber particles on mechanical properties and sustainability of ultra-high-ductile slag-based composites, Construction and Building Materials 272 (2021) 121959.
[34] Z. Luo, W. Li, K. Wang, S.P. Shah, D. Sheng, Nano/micromechanical characterisation and image analysis on the properties and heterogeneity of ITZs in geopolymer concrete, Cement and Concrete Research 152 (2022) 106677.
[35] G. Fang, W.K. Ho, W. Tu, M. Zhang, Workability and mechanical properties of alkali-activated fly ash-slag concrete cured at ambient temperature, Construction and Building Materials 172 (2018) 476-487.
[36] Y. Wang, Y. Wang, M. Zhang, Effect of sand content on engineering properties of fly ash-slag based strain hardening geopolymer composites, Journal of Building Engineering 34 (2021) 101951.
[37] M. Elchalakani, High strength rubberized concrete containing silica fume for the construction of sustainable road side barriers, Structures 1 (2015) 20-38.
[38] ASTM C1437-15, Standard Test Method for Flow of Hydraulic Cement Mortar, ASTM International, West Conshohocken, PA, United States, 2015.
[39] ASTM C642, Standard Test Method for Density, Absorption, and Voids in Hardened Concrete, ASTM International, West Conshohocken, PA, United States, 2013.
[40] ASTM C109/C109M-20b, Standard Test Method for Compressive Strength of Hydraulic Cement Mortars (Using 2-in . or [50-mm] Cube Specimens), ASTM International, West Conshohocken, PA, 2020.
[41] ASTM C1609, Standard Test Method for Flexural Performance of Fiber-Reinforced Concrete (Using Beam With Third-Point Loading), ASTM International, West Conshohocken, PA, United States, 2012.
[42] J.-D. Wu, L.-P. Guo, Y.-Z. Cao, B.-C. Lyu, Mechanical and fiber/matrix interfacial behavior of ultra-high-strength and high-ductility cementitious composites incorporating waste glass powder, Cement and Concrete Composites 126 (2022) 104371.

[43] S. Hesami, I. Salehi Hikouei, S.A.A. Emadi, Mechanical behavior of self-compacting concrete pavements incorporating recycled tire rubber crumb and reinforced with polypropylene fiber, Journal of Cleaner Production 133 (2016) 228-234.
[44] A.S. Eisa, M.T. Elshazli, M.T. Nawar, Experimental investigation on the effect of using crumb rubber and steel fibers on the structural behavior of reinforced concrete beams, Construction and Building Materials 252 (2020) 119078.
[45] M. Chen, H. Zhong, L. Chen, Y. Zhang, M. Zhang, Engineering properties and sustainability assessment of recycled fibre reinforced rubberised cementitious composite, Journal of Cleaner Production 278 (2021) 123996.
[46] R. Si, J. Wang, S. Guo, Q. Dai, S. Han, Evaluation of laboratory performance of self-consolidating concrete with recycled tire rubber, Journal of Cleaner Production 180 (2018) 823-831.
[47] A. Wongsa, V. Sata, B. Nematollahi, J. Sanjayan, P. Chindaprasirt, Mechanical and thermal properties of lightweight geopolymer mortar incorporating crumb rubber, Journal of Cleaner Production 195 (2018) 1069-1080.
[48] M. Abd Allah Abd-Elaty, M. Farouk Ghazy, O. Hussein Khalifa, Mechanical and thermal properties of fibrous rubberized geopolymer mortar, Construction and Building Materials 354 (2022) 129192.
[49] H. Zhong, E.W. Poon, K. Chen, M. Zhang, Engineering properties of crumb rubber alkali-activated mortar reinforced with recycled steel fibres, Journal of Cleaner Production 238 (2019) 117950.
[50] O. Youssf, M. Elchalakani, R. Hassanli, R. Roychand, Y. Zhuge, R.J. Gravina, J.E. Mills, Mechanical performance and durability of geopolymer lightweight rubber concrete, Journal of Building Engineering 45 (2022) 103608.
[51] S. Ramdani, A. Guettala, M.L. Benmalek, J.B. Aguiar, Physical and mechanical performance of concrete made with waste rubber aggregate, glass powder and silica sand powder, Journal of Building Engineering 21 (2019) 302-311.
[52] I. Mohammadi, H. Khabbaz, K. Vessalas, Enhancing mechanical performance of rubberised concrete pavements with sodium hydroxide treatment, Materials and Structures 49(3) (2016) 813-827.
[53] F. Ameri, P. Shoaei, H. Reza Musaeei, S. Alireza Zareei, C.B. Cheah, Partial replacement of copper slag with treated crumb rubber aggregates in alkali-activated slag mortar, Construction and Building Materials 256 (2020) 119468.
[54] S. Guo, Q. Dai, R. Si, X. Sun, C. Lu, Evaluation of properties and performance of rubber-modified concrete for recycling of waste scrap tire, Journal of Cleaner Production 148 (2017) 681-689.

[55] H. Wang, Y. Wu, B. Cheng, Mechanical properties of alkali-activated concrete containing crumb rubber particles, Case Studies in Construction Materials 16 (2022) e00803.
[56] A.M. Tahwia, M. Abd Ellatief, A.M. Heneigel, M. Abd Elrahman, Characteristics of eco-friendly ultra-high-performance geopolymer concrete incorporating waste materials, Ceramics International 48(14) (2022) 19662-19674.
[57] N.K. Lee, J.G. Jang, H.K. Lee, Shrinkage characteristics of alkali-activated fly ash/slag paste and mortar at early ages, Cement and Concrete Composites 53 (2014) 239-248.
[58] A. Alsaif, L. Koutas, S.A. Bernal, M. Guadagnini, K. Pilakoutas, Mechanical performance of steel fibre reinforced rubberised concrete for flexible concrete pavements, Construction and Building Materials 172 (2018) 533-543.
[59] J. Wang, Q. Dai, R. Si, S. Guo, Mechanical, durability, and microstructural properties of macro synthetic polypropylene (PP) fiber-reinforced rubber concrete, Journal of Cleaner Production 234 (2019) 1351-1364.
[60] M.M. Reda Taha, A.S. El-Dieb, M. Abd El-Wahab, M. Abdel-Hameed, Mechanical, fracture, and microstructural investigations of rubber concrete, Journal of materials in civil engineering 20(10) (2008) 640-649.
[61] M. Safan, F.M. Eid, M. Awad, Enhanced properties of crumb rubber and its application in rubberized concrete, Int. J. Curr. Eng. Technol 7(5) (2017) 1784-1790.
[62] R. Xiao, Z. Shen, R. Si, P. Polaczyk, Y. Li, H. Zhou, B. Huang, Alkali-activated slag (AAS) and OPC-based composites containing crumb rubber aggregate: Physico-mechanical properties, durability and oxidation of rubber upon NaOH treatment, Journal of Cleaner Production 367 (2022) 132896.
[63] K. Yu, H. Zhu, M. Hou, V.C. Li, Self-healing of PE-fiber reinforced lightweight high-strength engineered cementitious composite, Cement and Concrete Composites 123 (2021) 104209.
[64] K. Tharmaratnam, B.S. Tan, Attenuation of ultrasonic pulse in cement mortar, Cement and Concrete Research 20(3) (1990) 335-345.
[65] B. Ostle, Engineering statistics: the industrial experience, Wadsworth Publishing Company1996.
[66] B. Nematollahi, J. Sanjayan, F.U.A. Shaikh, Matrix design of strain hardening fiber reinforced engineered geopolymer composite, Composites Part B: Engineering 89 (2016) 253-265.